DOI: 10.1002/anie.201001077

$[An(H_2O)_9](CF_3SO_3)_3$ (An = U–Cm, Cf): Exploring Their Stability, Structural Chemistry, and Magnetic Behavior by Experiment and Theory**

Christos Apostolidis, Bernd Schimmelpfennig, Nicola Magnani, Patric Lindqvist-Reis, Olaf Walter, Richard Sykora, Alfred Morgenstern, Eric Colineau, Roberto Caciuffo, Reinhardt Klenze, Richard G. Haire, Jean Rebizant, Frank Bruchertseifer, and Thomas Fanghänel*

Dedicated to Professor Basil Kanellakopulos on the occasion of his 75th birthday

In recent years there has been considerable progress in understanding the chemistry of low-valent actinides and in the synthesis techniques for their compounds. A significant number of new compounds[1] has improved our knowledge about actinide–ligand bonds,[2] as well as establishing exciting, novel organouranium redox chemistry.[3] Progress has also been made in An^{3+}/Ln^{3+} (An = actinide; Ln = lanthanide) complexation and separation chemistry[4] and in the field of coordination and structural chemistry of hydrated An^{3+} ions in the solid state[5] and in solution.[5,6] Detailed information about the solution properties is essential, especially for predictions of actinide migration in natural aquifers near a nuclear waste repository. The aqueous chemistry of these An^{3+} ions is very similar to that of the Ln^{3+} ions; both are hard Lewis acids and interact mainly electrostatically with water, where their hydration numbers are governed largely by their ionic radii.

The decrease in the ionic radii across the An^{3+} series owing to the actinide contraction is believed to give rise to a change in the hydration numbers from nine to eight (between Cm^{3+} and Es^{3+}),[6] similar to that in the Ln^{3+} series.[7] This situation means that the corresponding decrease in the An−O bond lengths for these $An^{3+}(aq)$ ions across the series is slightly larger than the actual actinide contraction. A more appropriate structure probe for the actinide contraction would therefore be an isotypic series of crystalline compounds comprising $[An(H_2O)_9]^{3+}$ ions. To date, only three such compounds have been reported, $[An(H_2O)_9](CF_3SO_3)_3$ (An = Pu, Am, Cm),[5] which belong to the isotypic rare-earth triflate series, $[M(H_2O)_{9-x}](CF_3SO_3)_3$ (M = Ln, Y, Sc).[8,9] However, in contrast to the stable Ln^{III} triflates, the number of accessible An^{III} triflates is limited because Th^{3+} and Pa^{3+} are not stable in their trivalent states,[10] U^{3+} and Np^{3+} are extremely oxidation sensitive,[11] Cm^{3+}, Bk^{3+}, and Cf^{3+} are very scarce, and the transeinsteinium elements are too short-lived and do not exist in sufficient amounts. Recent attempts of obtaining $U(CF_3SO_3)_3$ by an earlier published method by treating UH_3 with neat triflic acid,[12a] resulted in oxidation and hydrolysis owing to traces of water in the acid.[12b] From those results it may be argued that **1**(U) is too unstable to be isolated; however, we show herein that this compound as well as **1**(Np) and **1**(Pu) are stable (even though the former two must be protected from air to avoid oxidation) and can be prepared from aqueous solutions in high yields. Herein, we report their synthesis, X-ray single-crystal structures along with that of **1**(Cf),[13] their electronic spectra and magnetic behavior. We also discuss their likeness to the Ln^{III} triflates and their significance as structural probes for $An^{3+}(aq)$, which we back up with two series of density functional theory (DFT)-optimized clusters, **2**(M) and **3**(M), the former of which mimic well the nona-hydrated cation structure in **1**(M), while the latter provide a reasonable model for nona-hydrated An^{3+} and Ln^{3+} aqua ions.

$[M(H_2O)_{9-x}](CF_3SO_3)_3$ **1**(M)
$M = An\ (U-Cm,\ Cf),\ Ln$

$[La(H_2O)_9]^{3+}\cdots[M(H_2O)_9\cdots(CF_3SO_3)_9]^{6-}\cdots[La(H_2O)_9]^{3+}$ **2**(M)
$M = An\ (Ac-Cf),\ Ln\ (La,\ Nd,\ Gd,\ Er,\ Lu)$

$[M(H_2O)_9]^{3+}\cdots(H_2O)_{18}$ **3**(M)
$M = An(Ac-Cf),\ Ln\ (La,\ Gd,\ Eu)$

---

[*] Dr. B. Schimmelpfennig, Dr. P. Lindqvist-Reis, Dr. R. Klenze
Institut für Nukleare Entsorgung, Karlsruhe Institute of Technology
P.O. Box 3640, 76021 Karlsruhe (Germany)
E-mail: patric.lindqvist@kit.edu

Dr. C. Apostolidis, Dr. N. Magnani, Dr. A. Morgenstern,
Dr. E. Colineau, Prof. Dr. R. Caciuffo, Dr. J. Rebizant,
Dr. F. Bruchertseifer, Prof. Dr. T. Fanghänel
European Commission, Joint Research Centre,
Institute for Transuranium Elements, Karlsruhe (Germany)

Dr. O. Walter
Institut für Technische Chemie, Karlsruhe Institute of Technology, Karlsruhe (Germany)

Dr. R. Sykora
Department of Chemistry, University of South Alabama, Mobile (USA)

Dr. R. G. Haire
Transuranium Research Laboratory, Chemical Sciences Division
Oak Ridge National Laboratory (USA)

[**] The authors are indebted for the use of ^{249}Cf produced by the HFIR at Oak Ridge National Laboratory.

Supporting information for this article is available on the WWW under http://dx.doi.org/10.1002/anie.201001077.

The synthesis scheme for **1**(U–Pu) was specially designed for obtaining single crystals of these oxidation-sensitive compounds in high yields, whereas a micro-preparation strategy was required for **1**(Cf) owing to the paucity and the hard gamma emission of ^{249}Cf. Although **1**(Pu) has also been obtained previously by dissolving Pu metal in dilute triflic acid followed by concentration and crystallization,[5a] this procedure failed for **1**(U) because of oxidation and hydrolysis problems.[12b] We avoided these problems by reducing higher oxidation states of the actinide ions to their trivalent states using zinc amalgam; the reduction is clearly seen by color change of the solutions (see the Supporting Information, Figure S1–S2). These solutions were then added to frozen triflic acid and the mixture slowly brought to room temperature to obtain deep-blue/purple crystals of **1**(U–Pu) (Supporting Information, Figure S3).

The coordination geometry of the $[M(H_2O)_9]^{3+}$ ions in **1**(M) is a tricapped trigonal prism (TTP) of C_{3h} symmetry, with six equidistant water oxygen atoms in the prismatic positions and three in the capping positions at markedly longer distances. Each of the nine water ligands donates two hydrogen bonds to the adjacent triflate anions (Figure 1a). This hydrogen-bond arrangement is the main reason for the C_{3h} symmetry, for the large difference between the prismatic and capping M–O distances, and for the particular orientation of the water ligands.[5,8,9] It is worth noting that the hydrogen bonding in **1**(M) is similar to that in $[M(H_2O)_9](H_5C_2SO_4)_3$,[14a] both of which feature almost identical stereochemistry of the hydrated cations. In contrast, owing to the different hydrogen-bond structure in $[M(H_2O)_9](BrO_3)_3$, the stereochemistry, local symmetry (D_{3h}), and M–O bond lengths are quite different.[14b] These conclusions are confirmed by the DFT-optimized clusters of **2**(M), where the inner $[M(H_2O)_9\cdots(CF_3SO_3^-)_9]^{6-}$ moieties mimic well that of the respective crystal structure (Figure 1b). Replacing the triflate ions in **2**(M) for water molecules we obtain the aqua-ion-like clusters of **3**(M), in which the capping water molecules are turned 90° with respect to their initial positions (the displacements of the prismatic water molecules are smaller), resulting in a change of the local symmetry of the $[M(H_2O)_9]^{3+}$ entity from C_{3h} to D_3 (Figure 1c). On the other hand, if we consider only their local MO_9 structure the two clusters are comparable. This result is supported by the similarity of the 5f electronic absorption spectra of **1**(U–Cm) and their respective aqueous solutions (see Figure S3a–c in the Supporting Information and Figures 3 and 4 in Ref. [5b]), which suggest a similar time-averaged coordination geometry of the aqua ions to that of the static TTP geometry in the crystals. In addition, in a recent extended X-ray absorption fine-structure (EXAFS) spectroscopy study it was shown that **1**(Ln) mimic well the first hydration spheres of the respective Ln^{3+}(aq) ions.[9c]

Figure 2a shows the prismatic and capping metal-oxygen distances in **1**(M). For the lanthanides the decrease in the prismatic distances along the series follows roughly the Ln^{3+} contraction.[8,15a] Only at the end of the series are deviations

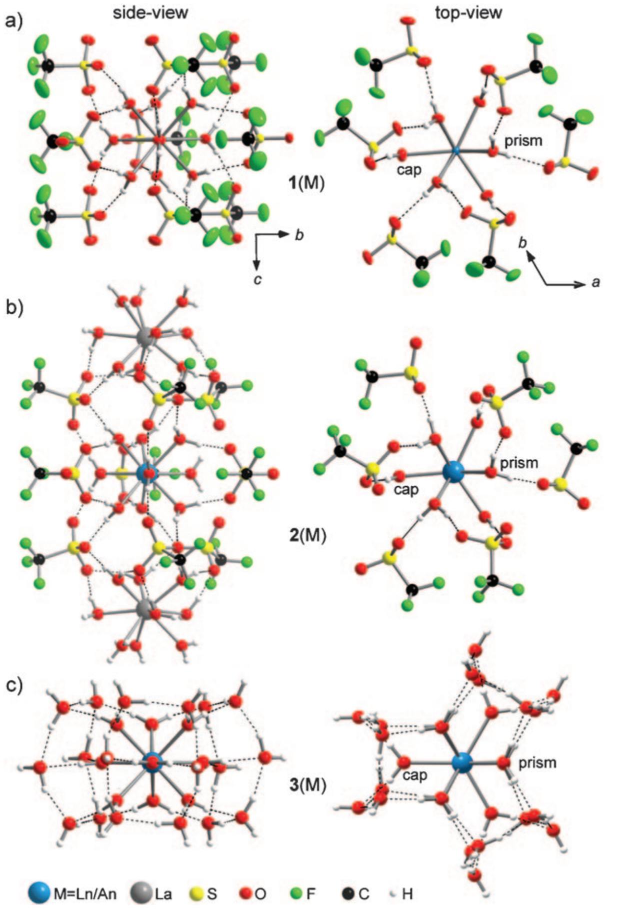

Figure 1. Molecular structures of a) the $[M(H_2O)_{9-x}\cdots(CF_3SO_3^-)_9]^{6-}$ entity in **1**(M) (thermal ellipsoids are set at 50% probability; T = 200 K), b) the $[La(H_2O)_9]^{3+}\cdots[M(H_2O)_9\cdots(CF_3SO_3^-)_9]^{6-}\cdots[La(H_2O)_9]^{3+}$ cluster of **2**(M) (in the top view the $[La(H_2O)_9]^{3+}$ entities are omitted for clarity), and c) the $M(H_2O)_9^{3+}\cdots(H_2O)_{18}$ cluster of **3**(M). In (a)–(c) the structures shown are for M = U.

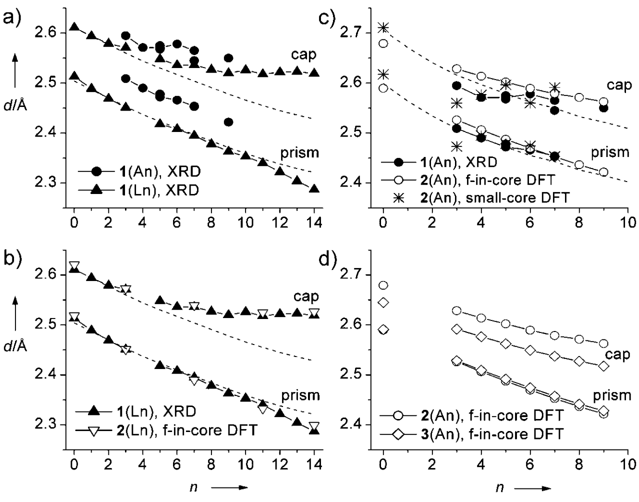

Figure 2. a)–d) Prismatic and capping M–O distances (d) in the $[M(H_2O)_9]^{3+}$ (M = Ln, An) ions of **1**(M), **2**(M), and **3**(An) (n = number of electrons in 4f or 5f orbitals). Distances calculated by DFT are overestimated. For comparison with experimental data, the theoretical values are offset by −0.058 Å for the f-in-core data and by −0.025 Å for the small-core data. The dashed lines show estimated Ln/An–O distances obtained by adding the Ln^{3+}/An^{3+} ionic radii[15a,b] to the water oxygen atom radius (2.34 Å).[15c]

from this trend apparent. The capping distances are approximately 0.1 Å longer than the prismatic ones in the beginning of the series, but this difference increases markedly in the second half of the series owing to the increasing steric crowding between the water ligands.[9b] For the actinides the prismatic and capping distances follow their lanthanide counterparts rather closely, although the capping distances in **1**(U) and **1**(Np) are slightly shorter (0.02 ± 0.005 Å). This shortening may be due to a minor contraction of the cell volume at 200 K, which seems to be the reason for the appreciably shorter capping distance in **1**(Cm) at 100 K (2.545(1) Å compared to 2.565(8) Å at 293 K).[5b,c] In the f-in-core DFT-optimized clusters of **2**(M) the prismatic and capping distances show similar trends as in the crystals (Figure 2b–c). This agreement is further improved for the lighter actinides by employing the small-core approximation (see Experimental Section for details). Particular good agreement is seen for the lanthanides, although the functional and the Ln/An f-in-core approximations slightly overestimate (0.06–0.07 Å) these distances. For the An–O distances in **2**(An) and **3**(An) the prismatic distances are identical for a given actinide (Ac–Cf), while the capping distances are longer in the **2**(An) series than in the **3**(An) (Figure 2d). Similar results were found for the Ln–O distances (not shown).

Temperature-dependent magnetic susceptibility data, $\chi(T)$, were collected for **1**(U–Am) in the 2–300 K range in an applied field of 1 T; the data are shown in Figure 3a for **1**(U) and **1**(Np) and in Figure S6 in the Supporting Information for **1**(Pu) and **1**(Am). The upturns in the $\chi(T)$ curves of **1**(Np) and **1**(Am) at low temperature were attributed to paramagnetic impurities; the overall behavior along the series is consistent with that expected for non-interacting An^{3+} ions. According to Hund's rules the Am^{3+} energy spectrum is characterized by a null total angular momentum $J = 0$. Hence, the non-magnetic behavior shown by the experimental curve is reasonable. The first magnetic states for Am^{3+} in **1**(Am) belong to the $^5F_1$ multiplet approximately 1740 cm^{-1} above the ground state, which is too high in energy to be populated, even at room temperature. Conversely, Np^{3+} in **1**(Np) can carry a magnetic moment since its low-energy multiplet is $^3H_4$; however, the fact that its susceptibility converges to a constant, finite value for $T \rightarrow 0$ K indicates that also in this case the ground state is non-magnetic. In fact, in the case of a non-Kramers ion (i.e., one with an even number of electrons in its unfilled shell, or equivalently with an integer J quantum number) a ligand field (LF) of low symmetry can split the low-energy J manifold in at most $2J+1$ levels, potentially removing the free-ion degeneracy to result in a non-magnetic singlet ground state. On the contrary, for the Kramers ions U^{3+} and Pu^{3+} time-even interactions, such as the LF, can only split a J (half-integer) manifold in at most $(2J+1)/2$ doublets, which in general carry a magnetic moment. This situation is consistent with the divergence of the susceptibility curves (and the Curie-like behavior, χ^{-1} linear in T) for **1**(U) and **1**(Pu) at low temperature. The magnetic susceptibilities of **1**(U–Am) can be quantitatively reproduced by ligand field calculations using an intermediate-coupling Hamiltonian and C_{3h} local symmetry (see the Supporting Information), which generate the energy level schemes shown in Figure 3b.

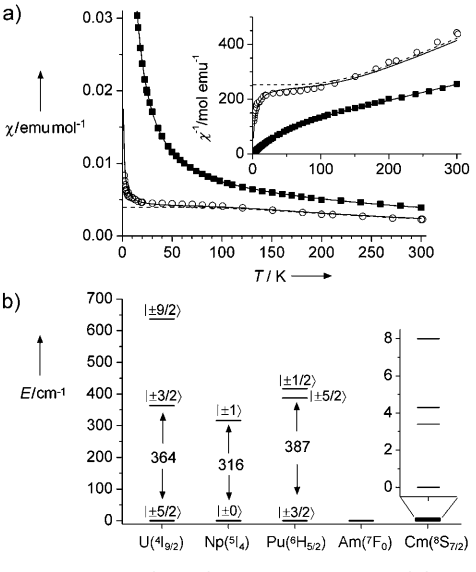

Figure 3. a) Temperature-dependent magnetic susceptibility and inverse of magnetic susceptibility (inset) for **1**(U) (■) and **1**(Np) (○), and their corresponding LF-calculated data (——). The small amount of paramagnetic impurity in **1**(Np) is accounted for by adding a C/T term to the susceptibility; the curve calculated without this term for is shown with a dashed line. b) The lowest-energy 5f spectra of **1**(U–Cm); the four-fold $^8S_{7/2}$ ground state splitting of Cm^{3+} in **1**(Cm) is assumed to be very similar to that of Cm^{3+} in **1**(La).[16]

In summary, we have reported the synthesis, crystal structures, and magnetic data of the isotypic six-member series **1**(U–Cm, Cf).[5,8] In terms of redox stability, **1**(Pu) is fairly stable whereas **1**(U, Np) are extremely sensitive to oxidation. Nevertheless these compounds could be obtained in high yields using a specially designed synthesis scheme. X-ray structure analysis and, for the later actinides, f-in-core DFT calculations showed that the $[Ln/An(H_2O)_9]^{3+}$ ions in **1**(Ln/An) are virtually identical for similar Ln^{3+}/An^{3+} radii, which reflects the electrostatic nature of the Ln/An–O bonds. For the lighter actinides though, the small-core approach gave more reliable data in better agreement with experiment. From these results we conclude that not only the heavier An^{3+} ions but also the lighter ones are lanthanide-like in their aqua complexes. The magnetic susceptibilities of **1**(U–Am) were fully reproduced by ligand field calculations from which the 5f electronic level structures could be derived. Finally, we note that **1**(U) may be an important alternative precursor to $UI_3(thf)_4$,[17a–c] UI_3,[17d,e] and $U(CF_3SO_3)_3$,[12a]; $UI_3(thf)_4$ has played a central role for the recent development in uranium coordination and organometallic chemistry.[1,3]

Experimental Section

Sample Preparation: All syntheses and manipulations of the ^{238}U, ^{237}Np, ^{242}Pu, ^{239}Pu, and ^{243}Am samples were performed in Ar-filled glove boxes at the Institute for Transuranium Elements, Karlsruhe. The ^{249}Cf sample was handled at the Transuranium Research laboratory, Oak Ridge National Laboratory. Identical procedures were used for the synthesis of **1**(U-Pu). 3% zinc amalgam (0.5 mL; prepared as in Ref. [18] from Zn and Hg of Puratronic (AlfaAesar) grades in 0.25 M HCF_3SO_3) was added to closable (Teflon cap) quartz cuvettes containing the An (2.5 mL, 20–30 mg; 0.08–0.12 mmol) in 1 M CF_3SO_3H (An = ^{238}U, ^{237}Np, ^{242}Pu; note that the starting An oxidation state may be U^{IV}/U^{VI}, $Np^{IV}/Np^{V}/Np^{VI}$, or Pu^{IV}/Pu^{VI}). After this step, the closed cuvette was shaken for several minutes, upon which reduction to An^{3+} took place almost instantly, as seen by the color changes (Supporting Information, Figure S1–S2). UV/Vis spectroscopy was used to check that the reductions to An^{3+}(aq) were complete (Supporting Information, Figure S3). The An^{3+} solutions were then added carefully to Schlenk tubes (precooled in liquid-nitrogen) containing Ar-degassed 80 % CF_3SO_3H to give a final acid concentration of 50 %. It is crucial that the acid is approximately 80 % since high concentrations generate an undesired exothermic reaction when mixed and could cause an oxidation of the An^{3+} ions produced. The solutions were brought to room temperature while the tubes were gently shaken. Color changes should not be observed during this step. Crystals grow slowly from these solutions. To recrystallize, crystals and the supernatant solutions were gently heated up to 50 °C to form clear colored solutions (U^{3+}(aq): dark green-purple; Np^{3+}(aq) and Pu^{3+}(aq): dark-purple). These solutions were then cooled slowly (3 h) in a water bath to room temperature, whereupon needle-like crystals of **1**(U–Pu) were formed. The crystals were washed with small aliquots of cold diethyl ether, followed by mild drying under vacuum (< 10 Torr). The **1**(Np) and **1**(Pu) compounds were nearly identical, dark-purple in color, while **1**(U) (as well as U^{3+}(aq)) had a dark green-purple tint (dark-green in sunlight and dark-purple in neon lights; see Supporting Information, Figures S1–S3). All the crystals were air-sensitive: **1**(U) oxidized within an hour, seen as a slight color change; **1**(Np) was stable for about a day before it turned from purple to green; and **1**(Pu) was stable. Owing to the scarcity and hard gamma emission of ^{249}Cf, a micro-preparation strategy was used for **1**(Cf). CF_3SO_3H (2 mL; ca. 10 %) was added to $^{249}Cf_2O_3$ powder (1 mg; 3.7×10^{-6} mol). A colorless solution was obtained after heating to approximately 80 °C. Large, pale green crystals of **1**(Cf) were obtained after slow evaporation of this solution at room temperature. All the **1**(An) salts were hygroscopic; **1**(U–Cf) are soluble in non-oxidizing, oxygen-free dilute acids, and in many organic Lewis base solvents (e.g. THF, DMSO, DMF, CH_3CN, pyridine). Further details of the experimental procedures, crystallographic studies,[13] UV/NIR/Vis, IR spectroscopy, and magnetic susceptibility data including LF calculations are given in the Supporting Information.

Computational details: a) The **2**(M) clusters were optimized under restriction to the C_{3h} point group at the Resolution-of-the-Identity (RI) DFT-level using the BP86-functional as implemented in the TURBOMOLE package.[19a–h] For H, C, O, F, S, and La^{3+} we used def2-TZVP basis sets in TURBOMOLE,[19i] and for La the corresponding large-core pseudopotential.[19j,k] For the An^{3+} we used the recently developed f-in-core pseudopotentials and corresponding basis sets of AVTZP-quality[19l] and the latest small-core pseudopotentials and corresponding segmented basis sets.[19m,n] By using pseudopotentials we include relativistic effects and by using the f-in-core approach we also avoid dealing with open-shell systems, thus allowing the calculations to be carried out on a Linux-cluster in single-node mode. For H, C, O, F, S, An^{3+} (small-core) and La^{3+} optimized auxiliary basis sets are provided with TURBOMOLE,[19o] while for An^{3+} with f-in-core we used auxiliary basis sets derived locally from the auxiliary basis set for La^{3+}. As La^{3+} has the same number and type of explicitly treated electrons, augmenting with further steep and diffuse functions (later tested on small model systems) was sufficient. The errors in the An–O distances arising from this approximation were negligible. The f-in-core approximation for An^{3+} leads to somewhat too long An–O distances compared to more rigorous approximations, but the main, rather systematic distance deviations derived from X-ray diffraction can be attributed to limitations of the BP86 functional employed. As pointed out in Ref. [19l], the f-in-core approach may be too crude for the earlier An^{3+} ions. We thus carried out calculations using the small-core approach for An^{3+} ions using otherwise the same basis sets for the other elements and the same functional as in the calculations with the f-in-core approach. It is not unambiguous which of the possible $5f^n$ configurations best represents the ground state; we investigated several possible configurations for each An^{3+} cluster. A more thorough study would require the inclusion of spin-orbit coupling. The occupation scheme, energies, and the An–O distances are given in Table S5 in the Supporting Information. The An–O distances in Figure 2c for the f-in-core data are those of the lowest energy configurations. Despite some scattering in the data, it is not evident that the lowest energy configuration is the right one. There is an overall better agreement with experiment for the lighter An^{3+} ions (especially for Np^{3+}) with the small-core than with the f-in-core approach. We thus confirm that the latter approach may lead to results of doubtful validity for the lighter An^{3+} ions as indeed seen for their complexation with N-donor ligands.[19p] b) For **3**(M) the same method, basis sets, and pseudopotentials were used as for **2**(M). The geometry was restricted to D_3, otherwise all the parameters were relaxed. Despite such a structure not being at a true minimum, this model is considered to be adequate for nine-coordinated aqua complexes with a highly symmetric second coordination shell.

Received: February 22, 2010

Keywords: actinides · coordination modes · hydrates · lanthanides

---

[1] M. Ephritikhine, *Dalton Trans.* **2006**, 2501–2516; W. J. Evans, S. A. Kozimor, *Coord. Chem. Rev.* **2006**, *250*, 911–935.

[2] The 5f electrons of the early An^{3+} ions may to some extent participate in bonding with soft donor ligands; see, A. J. Gaunt, B. L. Scott, M. P. Neu, *Angew. Chem.* **2006**, *118*, 1668–1671; *Angew. Chem. Int. Ed.* **2006**, *45*, 1638–1641; L. Karmazin, M. Mazzanti, J. Pécaut, *Chem. Commun.* **2002**, 654–655; J.-C. Berthet, Y. Miquel, P. B. Iveson, M. Nierlich, P. Thuéry, Ch. Madic, M. Ephritikhine, *J. Chem. Soc. Dalton Trans.* **2002**, 3265–3272.

[3] T. Cantat, C. R. Graves, B. L. Scott, J. L. Kiplinger, *Angew. Chem.* **2009**, *121*, 3735–3738; *Angew. Chem. Int. Ed.* **2009**, *48*, 3681–3684; O. P. Lam, C. Anthon, K. Mayer, *Dalton Trans.* **2009**, 9677–9691; O. T. Summerscales, G. F. N. Cloke, P. B. Hitchcock, J. C. Green, N. Hazari, *Science* **2006**, *311*, 829–831; I. Castro-Rodriguez, H. Nakai, L. N. Zakharov, A. L. Rheingold, K. Meyer, *Science* **2004**, *305*, 1757–1759; I. Castro-Rodriguez, H. Nakai, P. Gantzel, L. N. Zakharov, A. L. Rheingold, K. Meyer, *J. Am. Chem. Soc.* **2003**, *125*, 15734–15735.

[4] Z. Kolarik, *Chem. Rev.* **2008**, *108*, 4208–4252.

[5] a) J. H. Matonic, B. L. Scott, M. P. Neu, *Inorg. Chem.* **2001**, *40*, 2638–2639; b) P. Lindqvist-Reis, C. Apostolidis, J. Rebizant, A. Morgenstern, R. Klenze, O. Walter, T. Fanghänel, R. G. Haire, *Angew. Chem.* **2007**, *119*, 937–940; *Angew. Chem. Int. Ed.* **2007**, *46*, 919–922; c) S. Skanthakumar, M. R. Antonio, R. E. Wilson, L. Soderholm, *Inorg. Chem.* **2007**, *46*, 3485–3491.

[6] E. Galbis, J. Hernández-Cobos, C. den Auwer, C. Le Naour, D. Guillaumont, E. Simoni, R. R. Pappalardo, E. Sánchez Marcos, *Angew. Chem.* **2010**, *122*, 3899–3903; *Angew. Chem. Int. Ed.* **2010**, *49*, 3811–3815; B. Brendebach, N. L. Banik, M. Marquardt, J. Rothe, M. A. Denecke, H. Geckeis, *Radiochim. Acta* **2009**, *97*, 701–708; T. Stumpf, C. Hennig, A. Bauer, M. A. Denecke, T. Fanghänel, *Radiochim. Acta* **2004**, *92*, 133–138; M. R. Antonio, C. W. Williams, L. Soderholm, *Radiochim. Acta* **2002**, *90*, 851–856; P. G. Allen, J. J. Bucher, D. K. Shuh, N. M. Edelstein, I. Craig, *Inorg. Chem.* **2000**, *39*, 595–601; R. Revel, C. Den Auwer, C. Madic, F. David, B. Fourest, S. Hubert, J.-F. Le Du, L. R. Morss, *Inorg. Chem.* **1999**, *38*, 4139–4141.

[7] E. N. Rizkalla, G. R. Choppin in *Handbook on the Physics and Chemistry of Rare Earths. Lanthanides/Actinides: Chemistry,*

Vol. 18 (Eds.: K. A. Gschneidner, Jr., L. Eyring, G. R. Choppin, G. H. Lander), Elsevier Science, Amsterdam, **1994**, pp. 529–558.

[8] a) J. M. Harrowfield, D. L. Kepert, J. M. Patrick, A. H. White, *Aust. J. Chem.* **1983**, *36*, 483–492; b) C. O. Paiva Santos, E. E. Castellano, L. C. Machado, G. Vicentini, *Inorg. Chim. Acta* **1985**, *110*, 83–86; c) A. Chatterjee, E. N. Maslen, K. J. Watson, *Acta Crystallogr. Sect. B* **1988**, *44*, 381–386; d) C. Bisi Castellani, O. Carugo, M. Giusti, *Eur. J. Solid State Inorg. Chem.* **1995**, *32*, 1089–1099.

[9] a) The $[M(H_2O)_{9-x}](CF_3SO_3)_3$ (M = An, Ln, Y, Sc) salts crystallize in $P6_3/m$; however, vacancies occur for Er–Lu ($0 \leq x \leq 1$) and Sc ($x \approx 1$); see, b) A. Abbasi, P. Lindqvist-Reis, L. Eriksson, D. Sandström, S. Lidin, I. Persson, M. Sandström, *Chem. Eur. J.* **2005**, *11*, 4065–4077; c) I. Persson, P. D'Angelo, S. De Panfilis, M. Sandström, L. Eriksson, *Chem. Eur. J.* **2008**, *14*, 3056–3066.

[10] G. Ionova, C. Madic, R. Guillaumont, *Polyhedron* **1998**, *17*, 1991–1995.

[11] Few solid U^{III} hydrates have been characterized to date. These include various chloride, bromide, and sulfate salts; see, A. Mech, M. Karbowiak, T. Lis, J. Drożdżyński, *Polyhedron* **2006**, *25*, 2083–2092; J. Drożdżyński, *Coord. Chem. Rev.* **2005**, *249*, 2351–2373.

[12] a) J.-C. Berthet, M. Lance, M. Nierlich, M. Ephritikhine, *Eur. J. Inorg. Chem.* **1999**, 2005–2007; b) L. Natrajan, M. Mazzanti, J.-P. Bezombes, J. Pécaut, *Inorg. Chem.* **2005**, *44*, 6115–6121.

[13] CCDC 765808, CCDC 765809, CCDC 765810, CCDC 765811, and CCDC 765812 contain the supplementary crystallographic data for this paper. These data can be obtained free of charge from The Cambridge Crystallographic Data Centre via www.ccdc.cam.ac.uk/data_request/cif.

[14] a) R. E. Gerkin, W. J. Reppart, *Acta Crystallogr. Sect. C* **1984**, *40*, 781–786; b) J. Albertsson, I. Elding, *Acta Crystallogr. Sect. B* **1977**, *33*, 1460–1469.

[15] a) R. D. Shannon, *Acta Crystallogr. Sect. A* **1976**, *32*, 751–767; b) F. David, *J. Less-Common Met.* **1986**, *121*, 27–42; c) J. K. Beattie, S. P. Best, B. W. Skelton, A. H. White, *J. Chem. Soc. Dalton Trans.* **1981**, 2105–2111.

[16] P. Lindqvist-Reis, C. Walther, R. Klenze, N. M. Edelstein, *J. Phys. Chem. C* **2009**, *113*, 449–458.

[17] a) G. B. Deacon, T. D. Toung, *Polyhedron* **1988**, *7*, 249–250; b) D. L. Clark, A. P. Sattelberger, S. G. Bott, R. N. Vrtis, *Inorg. Chem.* **1989**, *28*, 1771–1773; c) L. R. Avens, S. G. Bott, D. L. Clark, A. P. Sattelberger, J. G. Watkin, B. D. Zwick, *Inorg. Chem.* **1994**, *33*, 2248–2256; d) W. J. Evans, S. A. Kozimor, J. W. Ziller, A. A. Fagin, M. N. Bochkarev, *Inorg. Chem.* **2005**, *44*, 3993–4000; e) C. D. Carmichael, N. A. Jones, P. L. Arnold, *Inorg. Chem.* **2008**, *47*, 8577–8589.

[18] G. Brauer, *Handbuch der Präparativen Anorganischen Chemie*, Bd. 3, F. Enke Verlag, Stuttgart, **1981**, pp. 2064–2065.

[19] a) P. A. M. Dirac, *Proc. R. Soc. London, Ser. A* **1929**, *123*, 714–733; b) J. C. Slater, *Phys. Rev.* **1951**, *81*, 385–390; c) S. H. Vosko, L. Wilk, M. Nusair, *Can. J. Phys.* **1980**, *58*, 1200–1211; d) J. P. Perdew, *Phys. Rev. B* **1986**, *33*, 8822–8824; e) A. D. Becke, *Phys. Rev. A* **1988**, *38*, 3098–3100; f) K. Eichkorn, O. Treutler, H. Öhm, M. Häser, R. Ahlrichs, *Chem. Phys. Lett.* **1995**, *242*, 283–290; Erratum: K. Eichkorn, O. Treutler, H. Öhm, M. Häser, R. Ahlrichs, *Chem. Phys. Lett.* **1995**, *242*, 652; g) K. Eichkorn, F. Weigend, O. Treutler, R. Ahlrichs, *Theor. Chim. Acta* **1997**, *97*, 119–124; h) TURBOMOLE V6.0, TURBOMOLE GmbH Karlsruhe, **2009**; http://www.turbomole.com; i) F. Weigend, R. Ahlrichs, *Phys. Chem. Chem. Phys.* **2005**, *7*, 3297–3305; j) M. Dolg, H. Stoll, A. Savin, H. Preuss, *Theor. Chim. Acta* **1989**, *75*, 173–194; k) M. Dolg, H. Stoll, H. Preuss, *Theor. Chim. Acta* **1993**, *85*, 441–450; l) A. Moritz, X. Cao, M. Dolg, *Theor. Chem. Acc.* **2007**, *117*, 473–481; m) X. Cao, M. Dolg, H. Stoll, *J. Chem. Phys.* **2003**, *118*, 487–496; n) X. Cao, M. Dolg, *J. Mol. Struct.* **2004**, *673*, 203–209; o) F. Weigend, *Phys. Chem. Chem. Phys.* **2006**, *8*, 1057–1065; p) N. L. Banik, B. Schimmelpfennig, C. M. Marquardt, B. Brendebach, A. Geist, M. A. Denecke, *Dalton Trans.* **2010**, 5117–5122.